PHYSICAL REVIEW B **90**, 220507(R) (2014)

Threshold of magnetic field response of the superconducting proximity effect for ultrathin Pb/Ag metallic films

M. Caminale,[1] A. A. Leon Vanegas,[1,2] A. Stępniak,[1] H. Oka,[1] D. Sander,[1,*] and J. Kirschner[1,2]

[1]*Max-Planck-Institut für Mikrostrukturphysik, Weinberg 2, 06120 Halle, Germany*

[2]*Institut für Physik, Martin-Luther-Universität Halle-Wittenberg, 06120 Halle, Germany*

(Received 20 June 2014; revised manuscript received 21 November 2014; published 5 December 2014)

The proximity effect describes the extension of superconductivity into a metal, which is in contact with a superconductor. Scanning tunneling spectroscopy is used to probe this effect in a two-atomic-layer Pb/Ag nonsuperconducting film, surrounding a superconducting Pb nanoisland, with sub-nm spatial resolution. Here we show a nontrivial dependence of the length scales of the superconducting proximity effect on magnetic field. Surprisingly, we find that the magnetic field does not affect the induced superconductivity up to 0.3 T, but a breakdown of the proximity effect is induced for fields around 0.6 T, with a $1/H^p$ dependence with $p \cong 7$. The unexpected robustness of the induced superconductivity in the presence of magnetic fields is ascribed to the high electronic diffusivity in the metallic wetting layer.

DOI: 10.1103/PhysRevB.90.220507 PACS number(s): 74.45.+c, 74.25.Op

The intriguing possibility to induce superconductivity in a metal (M), in direct contact with a superconductor (S), has lately seen renewed intense interest from both application and fundamental points of view [1–11]. This interest is spurred by improvements in nanofabrication for the development of future superconducting devices, and by the employment of low temperature scanning tunneling microscopy/spectroscopy (STM/STS) as a tool to visualize how superconductivity extends spatially in M. The underlying phenomenon is commonly known as the proximity effect. The proximity effect is characterized by the *proximity length*, on which a superconducting gap in the local density of states (LDOS) of M fades out with distance from S [2,9–14]. The effect is usually depicted in terms of induced correlated pairs in M [2,4,5,11,14], which originate from a leaking of Cooper pairs from S, by means of Andreev reflections [1,11]. A fundamental outstanding question is how the induced superconducting properties and their extension respond to the application of an external magnetic field. To the best of our knowledge, only one non-spatially-resolved magnetoresistance study has been reported so far, for a micrometer-long Au wire between two superconducting electrodes [5]. Recent STM/STS studies have revealed induced superconductivity extending over 15–40 nm in zero field, for a Pb ultrathin film surrounding superconducting Pb islands [9–11]. Further in-field STM/STS measurements focused exclusively on the vortex formation in superconducting Pb nanoislands [15–19].

Here, we report a STM/STS study on the magnetic field dependence of the spatial extension of the proximity-induced superconductivity. We study the proximity effect in a nonsuperconducting Pb/Ag wetting layer surrounding a superconducting Pb nanoisland. Differential conductance measurements characterize the LDOS of the metallic film as a function of the distance from the superconducting island, for different magnetic fields along the surface normal. We observe a gap in the conductance spectra, which we ascribe to induced superconductivity, and this spectral feature is observed over 25 nm from the edge of the superconducting island, in zero field. Our experiments unveil a nontrivial response of the proximity length to field: Surprisingly, the proximity length is fairly unaffected by magnetic fields up to 0.3 T, revealing an unexpected robustness of the induced superconductivity in the Pb/Ag film, even far from the superconducting island. Applying out-of-plane fields up to 0.6 T, a change of the decay of the proximity length is measured. We establish that this change is related to the variation of the conductance at zero bias at the island edge. For larger fields, we observe a steep decrease of the proximity length proportional to H^{-p}, with $p \cong 7$.

The experiments were performed in an ultrahigh vacuum chamber with a ^{3}He-cooled STM equipped with a vector magnetic field [20]. The Pb/Ag system is prepared on an *n*-type doped Si(111) single crystal by *in situ* molecular beam epitaxy in three steps [20]. First, one atomic layer of Ag is evaporated at 770 K on the atomically clean 7×7-Si(111) surface reconstruction [21]. Deposition of Ag lifts the 7×7 reconstruction, and Ag covers the surface with a regular $\sqrt{3} \times \sqrt{3}$ structure [22,23]. Subsequently a little more than one atomic layer of Pb is evaporated at room temperature, followed by annealing at 550 K for 1 min. This leads to the formation of an ordered Pb/Ag film showing patches of a $\sqrt{3} \times \sqrt{3}$ and a $\sqrt{3} \times \sqrt{7}$ structure. Finally, a further deposition of 1.6 monolayer (ML) Pb at 240 K at a rate of 3 min/ML leads to the formation of Pb islands on the Pb/Ag wetting layer. These growth conditions lead to the predominant formation of Pb islands of 9 ML height [24]. Figure 1(a) shows a constant-current STM image of a 9 ML high Pb island on the wetting layer. The island thickness is independently determined by STS of quantum well states [25] (see Supplemental Material S1 [26]). The island exhibits atomically flat surfaces of different heights, characterized by nm large and one-atomic-layer high depressions and mesas [24,27]. On the contrary, the Pb/Ag wetting layer has a rough surface on the nm scale due to Pb clusters formed during island growth. The Pb island is superconducting with a critical temperature T_c of ∼6.1 K, as inferred from the plot of the superconducting gap Δ as a function of temperature in the inset of Fig. 1(a) (see Supplemental Material S2 [26]).

*sander@mpi-halle.mpg.de

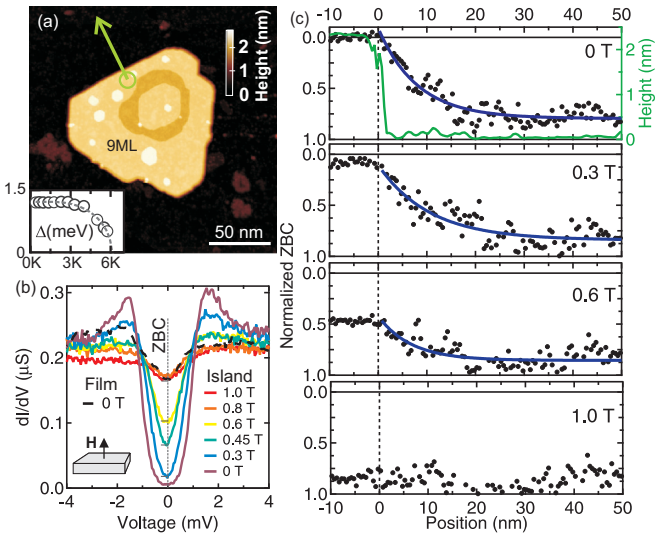

FIG. 1. (Color online) (a) Constant-current STM image of a Pb island on Pb/Ag/Si(111). The inset shows the superconducting gap Δ as a function of temperature; the dashed line is a fit from the BCS density of states. (b) Point spectroscopy of the differential conductance taken on the island edge [green circle in (a)] at different out-of-plane fields (see the sketch) at 1.75 K. The spectrum of the normal state of the Pb/Ag wetting layer far from the island is also reported as a reference (black dashed curve). The tunneling junction was stabilized at 10 mV bias voltage and 1 nA tunneling current. (c) Normalized zero-bias conductance NZBC (black markers) as a function of position from the Pb island (negative values) to the Pb/Ag film (positive values) along the green arrow in (a) at 1.75 K, for different magnetic fields. The top panel shows also the corresponding constant-current line scan for clarity. The definition of NZBC is given in the text. The blue curves represent an exponential fit which gives the proximity length γ; see text for details. Note that the NZBC axis counts positive downwards.

STS on the Pb/Ag wetting layer showed no indications of superconductivity down to 0.38 K (see Supplemental Material S2–S3 [26]).

Figure 1(b) shows the differential conductance (dI/dV) spectra taken on the island close to its edge [green circle in Fig. 1(a)] at 1.75 K, for increasing magnetic fields along the surface normal. In-plane fields do not change the differential conductance spectrum of the superconducting island up to the highest experimental value of 1.4 T. Without field (0 T), the spectrum exhibits a clear gap centered at zero bias, where the differential conductance drops to zero. With increasing field, the gap is gradually smeared out and an increase of the zero-bias conductance [ZBC, as depicted in Fig. 1(b)] is observed up to 0.8 T. The spectra remain constant with increasing field up to 4 T. We conclude that magnetic fields above the critical value $H_{c2} = 0.8$ T suppress superconductivity, and the island turns to its normal state. Given an effective radius $r_{\text{eff}} \gtrsim 40$ nm ($r_{\text{eff}} = \sqrt{\frac{S}{\pi}}$, where S is the island area), a vortex appears in the center of the island at a field $H_{c1} < H_{c2}$ [15–17] (see Supplemental Material S4 [26]). The differential conductance spectrum of the normal state shows a small dip around zero bias. A comparable spectroscopic feature has been previously reported for Pb islands, as well as on different substrates [28,29]. The spectrum of the normal state of the Pb/Ag wetting layer far from the island, at 0 T, is also reported for comparison ["Film," Fig. 1(b)]. Note that in the normal state both the island and the wetting layer show the same value of conductance at zero bias. These observations identify the dip in the differential conductance as a characteristic of nanoscale Pb systems, unrelated to superconductivity [10,28,29]. The data in Fig. 1(b) show a clear rise of the ZBC from 0 with increasing out-of-plane field. This indicates a field-driven weakening of the superconducting condensate in the island. In the following, we take the normalized value of the conductance at zero bias (NZBC) as an indicator of the superconductivity of the island [2,9,15,16]. The NZBC is calculated by dividing the measured ZBC value by the conductance at 5 mV, far from the gap area; the normal state is identified by NZBC = 0.8.

We next turn to the main result of our work. We investigate the extension of the induced superconductivity in the metallic film by analyzing the spatial dependence of the ZBC from a straight edge of a superconducting island. Figure 1(c) shows the normalized zero-bias conductance (NZBC) at 1.75 K along a straight line from the Pb island to the Pb/Ag wetting layer, for increasing magnetic fields. In Fig. 1(a) the green arrow depicts the measurement direction and the corresponding topographic line scan is displayed in the top panel of Fig. 1(c). For 0 T [Fig. 1(c), top panel], the NZBC remains 0 up to the island edge, and then it gradually changes towards 0.8 within a proximity length of about 25 nm from the edge. We use this measurement at 0 T to characterize the wetting layer in the framework of the Usadel description for the electronic DOS in S-M junctions [2,9,10,13,14]. Within this picture, Cooper pairs diffuse from S to M, and the proximity length is mainly determined by intrinsic electron scattering processes, characterized by the value of the diffusivity constant D. The evolution of the NZBC with the distance from the boundary indicates an electron diffusivity $D \sim 1\ \text{cm}^2/\text{s}$ of the Pb/Ag (see Supplemental Material S5 [26]), in agreement with previous publications [10]. This characterizes the wetting layer as a so-called highly diffusive metal [2,10]. With increasing field, the NZBC at the island edge rises, and in the wetting layer the normal-state value of the NZBC is reached already 10 nm away from the edge at 0.6 T. At 1 T, the island is in its normal state [Fig. 1(b)], and a constant NZBC with no distinct spatial dependence is measured. In-plane fields up to the largest experimental value of 1.4 T do not affect the proximity-induced superconductivity. Note that no spatial variation of the NZBC value from the edge towards the inner island is observed within our experimental sensitivity. Previous works on comparable lateral S-M junctions report a very mild weakening of the superconducting counterpart near the boundary with the metallic film [9,11]. This phenomenon, known as the *inverse* proximity effect, was accessible by analyzing the width of the superconducting gap with high energy resolution. Both geometrical [9] and electronic density [11] considerations were proposed to explain the remarkably tiny effect. We observe that the NZBC changes continuously at the edge. This indicates a transparent potential barrier between Pb and the wetting layer, in the framework of the Usadel description [14].

The spatially resolved measurement of the ZBC in magnetic field, described above, was performed on six islands, characterized in Table I. All islands show a comparable gap Δ of 1.2–1.3 meV at 1.75 K and a continuous transition of the

TABLE I. (Color online) Properties of the Pb islands: effective radius $r_{\text{eff}} = \sqrt{\frac{S}{\pi}}$; BCS-$\Delta$ at the measurement temperature 1.75 K; magnetic field H_{c1} for the onset of vortex formation and critical field H_{c2} of the island. Each island is identified by a different marker and color. The green line in the topography images indicates the line along which the spatially resolved measurements were performed. Island (i) is the one of Fig. 1(a). Island labels are as in Figs. 2 and 3.

140nm × 140nm						
Island label	*(i)* □	*(ii)* ▽	*(iii)* ○	*(iv)* ◇	*(v)* ⋈	*(vi)* ×
r_{eff} [nm]	57	56	55	55	33	21
Δ(1.75K) [meV]	1.24 ±0.02	1.19 ±0.02	1.33 ±0.03	1.27 ±0.02	1.31 ±0.02	1.18 ±0.04
H_{c1} [T]	0.48 ±0.05	0.45 ±0.05	0.55 ±0.05	0.38 ±0.05	*no vortex*	*no vortex*
H_{c2} [T]	0.80 ±0.05	0.80 ±0.05	1.15 ±0.05	1.15 ±0.05	1.25 ±0.05	1.70 ±0.05

ZBC from the island edge towards its surrounding. Smaller islands exhibit larger critical fields H_{c2} [15], allowing one to investigate the proximity effect in larger fields. For islands (v) and (vi) ($r_{\text{eff}} < 40$ nm) no vortex formation is observed [15].

In order to characterize how the external field affects the spatial dependence of the proximity-induced superconductivity, we introduce the proximity length γ. γ is defined by the fit of the position-dependent NZBC with the exponential function $A - Be^{-\frac{x}{\gamma}}$ [blue curves in Fig. 1(c)], for fields below H_{c2}. The parameter A is constrained to the value of the NZBC in the wetting layer in its normal state.

We plot the values of γ (left y axis) and of NZBC (right y axis) at the island edge as a function of the magnetic field in Fig. 2, for every island investigated. The NZBC (solid black data points) remains constant within 10% for fields smaller than 0.3 T. In larger fields the NZBC evolves towards the normal-state value. The value of γ (open data points) is of about 9.5 nm for all islands at 0 T, and it qualitatively follows the NZBC trend. Up to 0.3 T, γ remains fairly constant, then it decreases with increasing field. This analysis reveals that, surprisingly, fields below 0.3 T do not destroy the induced superconductivity even far away from the superconducting island. In addition, a reduction of the proximity length γ is observed only when the NZBC value at the island edge increases significantly.

These findings are rationalized by considering the effect of an external magnetic field on a superconducting condensate. In general, as described by the Meissner effect in bulk superconductors, a magnetic field induces superconducting shielding currents. However, the small lateral size of the nanoislands, in comparison to the much larger London penetration depth (≈3 μm in 10 ML Pb film [16]), leads to incomplete expulsion of the magnetic field. Both the field and the screening currents contribute to weaken the superconducting condensate. Their effect is considered in a so-called depairing energy parameter in the Cooper pair potential [13,30]. A reduced pair potential affects the superconducting gap in the LDOS across the superconductor, and a rise of the conductance at zero bias (ZBC) is observed [16]. A rise of the ZBC value in this context implies therefore a larger depairing energy. Since up to 0.3 T no variation of the proximity length γ, and hence no increase of the ZBC, is observed, we conclude that no depairing contribution is operative in the metallic film, at any distance from the island edge. This is an unexpected result for the induced superconductivity in our Pb/Ag film. Indeed, a superconducting Pb/Si(111) film of comparable thickness turns to the normal state with an out-of-plane field of about 0.15 T [20,31]. Fields in excess of 0.3 T cause a sizable rise of the ZBC at the edge, induced by the depairing action of the shielding currents [16]. Weaker correlated pairs are therefore induced in the film, and, as a result, a decay of the proximity length is observed.

To elucidate the relation between the proximity length γ and the conductance at zero bias at the island edge, we plot γ as a function of NZBC in Fig. 3(a), for all islands given in Table I. For NZBC below 0.1 (i.e., for fields below 0.3 T) the points cluster together. This confirms that, surprisingly, the application of external magnetic fields up to 0.3 T does not affect the proximity-induced superconductivity. The proximity length γ decreases with increasing NZBC. We conclude that γ depends on both D and NZBC(H):

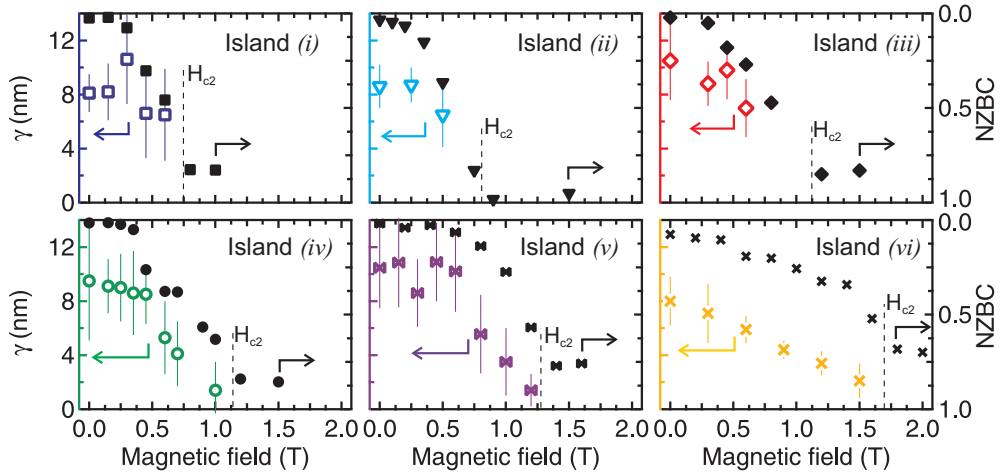

FIG. 2. (Color online) Proximity length γ (colored data points, left scale) and NZBC at the island edge (black data points, right scale) as a function of magnetic field for every island in Table I. Note that the NZBC axis counts positive downwards.

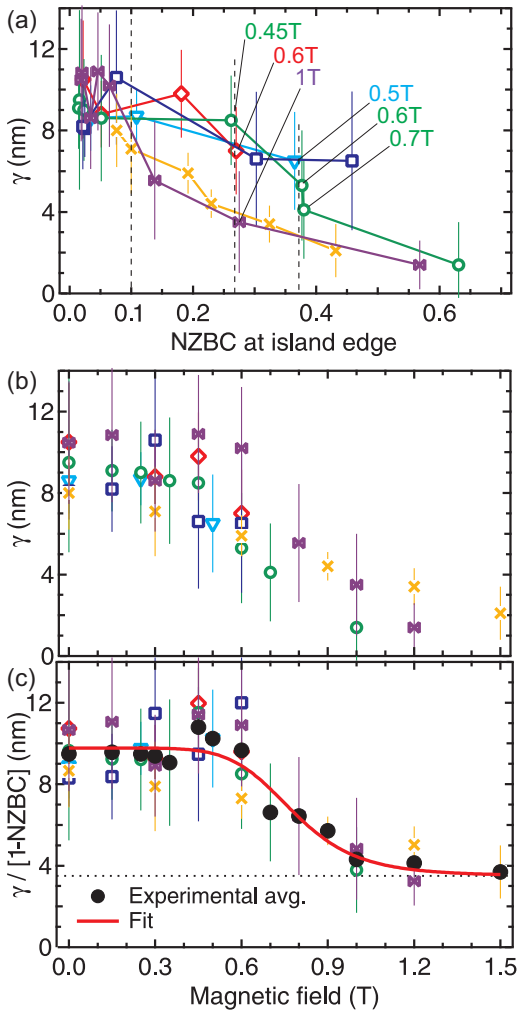

FIG. 3. (Color online) (a), (b) Proximity length γ as a function of the NZBC at the island edge and as a function of the applied magnetic field, respectively, for all the islands in Table I. (c) Ratio $[\gamma/(1-\mathrm{NZBC})]$ as a function of the magnetic field. Black solid markers are obtained averaging the experimental points for a given value of field. The red solid line results from a fit (for details, see the text).

$\gamma \to \gamma(D,\mathrm{NZBC}(H))$, where the diffusivity constant D represents electronic scattering processes in the wetting layer and the NZBC(H) accounts for the superconducting state of the island. Interestingly, the evolution of γ with NZBC follows different trends for different islands. In particular, we notice that for a given value of the NZBC (e.g., 0.26), a wide range of γ (4–9 nm) is found, where smaller values always correspond to larger applied fields. This suggests a more complex role played by the field in affecting the proximity effect. The dependence of the proximity length γ on the magnetic field is investigated next.

In Fig. 3(b) we present the values of γ as a function of field for every island investigated. Up to 0.3 T (i.e., for NZBC $<$ 0.1), the proximity length γ does not vary with field within the error bars. In larger fields, the points spread differently. The variation of γ with field is mainly determined by the evolution of the NZBC at the island edge. In order to extract the effect of the magnetic field on the induced superconductivity in the metal, we compare the evolution of γ and of the NZBC as a function of field, by plotting the ratio $R = \frac{\gamma}{1-\mathrm{NZBC}}$ (which is calculated for each island from the curves in Fig. 2) in Fig. 3(c). Remarkably, all points collapse into a single curve and follow a common trend. The black solid markers are the averaged value of the points for all the islands at the given field. Starting from 0 T, the ratio R is fairly constant up to 0.6 T. In larger fields, it decreases steeply and saturates at a constant value. The data points do not reach zero due to an experimental artifact, coined the "shadow effect" in previous works [10]. Due to the finite radius of the STM tip apex [when the tip in close proximity (2–4 nm) to the island edge], the tunneling spectra are dominated by the LDOS of the island facet facing the lateral side of the tip apex. The constant saturation value of R results from this shadow effect. The observed change of slope of R with field in Fig. 3(c) identifies two regimes for γ. Up to 0.6 T, the proximity length γ is given by the weakening of the superconducting condensate in the island. In addition, fields above 0.6 T contribute directly to a decay of the induced superconductivity, by field-driven depairing effects in the metal. We speculate that for fields in excess of 0.6 T, shielding currents appear also in the metallic film, albeit with a higher density as compared to the island, because of the factor of five smaller thickness. These currents induce a strong depairing, and hence a breakdown of the already weakened induced superconductivity.

The nontrivial behavior of the ratio $R = \frac{\gamma}{1-\mathrm{NZBC}}$ shown in Fig. 3(c) can be accounted for by ascribing the proximity length γ to a combination of two independent decay processes as follows :

$$\frac{1}{\gamma} \to \frac{1}{\gamma_{\mathrm{i}}(D,\mathrm{NZBC}(H))} + \frac{1}{\gamma_{\mathrm{H}}(H)},$$

where $\gamma_{\mathrm{i}}(D,\mathrm{NZBC}(H))$ is an intrinsic decay length as introduced before, while $\gamma_{\mathrm{H}}(H)$ includes the effect of the field on the decay of the proximity effect in the wetting layer. The ratio R in Fig. 3(c) can therefore be qualitatively fitted by a function:

$$R = \frac{\gamma(D,\mathrm{NZBC},H)}{1-\mathrm{NZBC}} \approx \left(\frac{1}{\gamma_{\mathrm{R0}}} + \frac{1}{A/H^{p}}\right)^{-1} + \gamma_{\mathrm{R1}}.$$

Here, A and p are free parameters of the fit and define $\gamma_{\mathrm{H}} \propto \frac{A}{H^{p}}$, while γ_{R0} and γ_{R1} are determined from the experimental data by $R(0\ \mathrm{T}) = \gamma_{\mathrm{i}}(0\ \mathrm{T}) = 9.5$ nm and $R(\infty) = \gamma_{\mathrm{R1}} = 3.5$ nm, respectively. The best fit [solid line in Fig. 3(c)] is obtained for $A = 1.1 \pm 0.5$ nm T^{p} and $p = 7.3 \pm 1.5$.

Our results provide a different picture for the magnetic response of the proximity effect, in comparison with the magnetoresistance study on a S-M-S junction in Ref. [5]. There, a breakdown of the induced superconductivity in the middle region of a micrometer-long Au wire was reported at a field of 0.25 T. In contrast to this previous work, we provide spatially resolved data which do not show a direct field-driven depairing up to 0.6 T. This points to a different response of the correlated pairs induced in the film to the application of an external magnetic field. We ascribe this unexpected behavior to the highly diffusive nature of the ultrathin Pb/Ag wetting layer studied here, where the intrinsic electronic scattering processes in the film dominate the proximity effect.

In conclusion, our work reveals the complex role of magnetic field in defining the length scales of the proximity effect in a lateral S-M system on the nanoscale. Applying out-of-plane magnetic fields, we probed the induced superconductivity in a Pg/Ag metallic wetting layer in proximity to superconducting Pb islands by position-resolved tunneling conductance measurements. We found that, unexpectedly, the proximity effect is unaffected up to 0.3 T, indicating that no field-driven depairing processes are active in the induced superconductivity. With increasing field above 0.3 T, a shorter proximity length is measured. This shows the possibility to indirectly affect the proximity length by tuning the superconductivity of S through an external magnetic field. Finally, from our analysis we extract an effect of the external magnetic field on the induced superconductivity, identifying a breakdown of the proximity effect above 0.6 T. The remarkably high breakdown field is ascribed to the high electronic diffusivity of the wetting layer. Our results contribute insights into the field dependence of the superconducting proximity effect. Our study provides a quantitative basis for future experimental investigations about the unexpected robustness, against a magnetic field, of the proximity effect in highly diffusive systems.

We acknowledge Dr. A. Sanna, Halle, and Dr. C. Winkelmann, Grenoble, for fruitful discussions and W. Greie for technical support. The work was partially supported by the DFG SFB 762 (Germany).

[1] H. Courtois, P. Gandit, and B. Pannetier, Phys. Rev. B **52**, 1162 (1995).
[2] S. Guéron, H. Pothier, N. O. Birge, D. Esteve, and M. H. Devoret, Phys. Rev. Lett. **77**, 3025 (1996).
[3] J. Xiang, A. Vidan, and M. Tinkham, Nat. Nanotechnol. **1**, 208 (2006).
[4] H. le Sueur, P. Joyez, H. Pothier, C. Urbina, and D. Esteve, Phys. Rev. Lett. **100**, 197002 (2008).
[5] J. Wang, C. Shi, M. Tian, Q. Zhang, N. Kumar, J. K. Jain, T. E. Mallouk, and M. H. W. Chan, Phys. Rev. Lett. **102**, 247003 (2009).
[6] F. Giazotto, J. Peltonen, M. Meschke, and J. Pekola, Nat. Phys. **6**, 254 (2010).
[7] J. E. Sadleir, S. J. Smith, S. R. Bandler, J. A. Chervenak, and J. R. Clem, Phys. Rev. Lett. **104**, 047003 (2010).
[8] M. Singh, J. Wang, M. Tian, T. E. Mallouk, and M. H. W. Chan, Phys. Rev. B **83**, 220506(R) (2011).
[9] J. Kim, V. Chua, G. A. Fiete, H. Nam, A. H. MacDonald, and C.-K. Shih, Nat. Phys. **8**, 464 (2012).
[10] L. Serrier-Garcia, J. C. Cuevas, T. Cren, C. Brun, V. Cherkez, F. Debontridder, D. Fokin, F. S. Bergeret, and D. Roditchev, Phys. Rev. Lett. **110**, 157003 (2013).
[11] V. Cherkez, J. C. Cuevas, C. Brun, T. Cren, G. Ménard, F. Debontridder, V. S. Stolyarov, and D. Roditchev, Phys. Rev. X **4**, 011033 (2014).
[12] P.-G. de Gennes, *Superconductivity of Metals and Alloys* (Benjamin, New York, 1966).
[13] K. Usadel, Phys. Rev. Lett. **25**, 507 (1970).
[14] W. Belzig, C. Bruder, and G. Schön, Phys. Rev. B **54**, 9443 (1996).
[15] T. Nishio, T. An, A. Nomura, K. Miyachi, T. Eguchi, H. Sakata, S. Lin, N. Hayashi, N. Nakai, M. Machida *et al.*, Phys. Rev. Lett. **101**, 167001 (2008).
[16] T. Cren, D. Fokin, F. Debontridder, V. Dubost, and D. Roditchev, Phys. Rev. Lett. **102**, 127005 (2009).
[17] T. Cren, L. Serrier-Garcia, F. Debontridder, and D. Roditchev, Phys. Rev. Lett. **107**, 097202 (2011).
[18] J. Kim, G. A. Fiete, H. Nam, A. H. MacDonald, and C.-K. Shih, Phys. Rev. B **84**, 014517 (2011).
[19] T. Tominaga, T. Sakamoto, H. Kim, T. Nishio, T. Eguchi, and Y. Hasegawa, Phys. Rev. B **87**, 195434 (2013).
[20] A. Stępniak, A. Leon Vanegas, M. Caminale, H. Oka, D. Sander, and J. Kirschner, Surf. Interface Anal. **46**, 1262 (2014).
[21] B. S. Swartzentruber, Y. W. Mo, M. B. Webb, and M. G. Lagally, J. Vac. Sci. Technol. A **7**, 2901 (1989).
[22] N. Sato, T. Nagao, and S. Hasegawa, Surf. Sci. **442**, 65 (1999).
[23] H. Aizawa, M. Tsukada, N. Sato, and S. Hasegawa, Surf. Sci. **429**, L509 (1999).
[24] M. Hupalo, V. Yeh, L. Berbil-Bautista, S. Kremmer, E. Abram, and M. C. Tringides, Phys. Rev. B **64**, 155307 (2001).
[25] M. C. Yang, C. L. Lin, W. B. Su, S. P. Lin, S. M. Lu, H. Y. Lin, C. S. Chang, W. K. Hsu, and T. T. Tsong, Phys. Rev. Lett. **102**, 196102 (2009).
[26] See Supplemental Material at http://link.aps.org/supplemental/10.1103/PhysRevB.90.220507 for independent measurement of the island thickness, temperature dependent spectroscopy, visualization of the vortex formation in the islands, and determination of the diffusivity constant *D*.
[27] F. Palmino, Ph. Dumas, Ph. Mathiez, C. Mouttet, F. Salvan, and U. Köhler, Ultramicroscopy **42-44**, 928 (1992).
[28] K. Wang, X. Zhang, M. M. T. Loy, T.-C. Chiang, and X. Xiao, Phys. Rev. Lett. **102**, 076801 (2009).
[29] C. Brun, K. H. Müller, I.-P. Hong, F. Patthey, C. Flindt, and W.-D. Schneider, Phys. Rev. Lett. **108**, 126802 (2012).
[30] A. Anthore, H. Pothier, and D. Esteve, Phys. Rev. Lett. **90**, 127001 (2003).
[31] T. Zhang, P. Cheng, W.-J. Li, Y.-J. Sun, G. Wang, X.-G. Zhu, K. He, L. Wang, X. Ma, X. Chen *et al.*, Nat. Phys. **6**, 104 (2010).